Mathematical Biosciences and Engineering

http://www.aimspress.com/journal/mbe

MBE, 19(3): 2835–2852.
DOI: 10.3934/mbe.2022130
Received: 14 November 2021
Revised: 16 December 2021
Accepted: 26 December 2021
Published: 13 January 2022

Research article

Global dynamics for a Filippov system with media effects

Cunjuan Dong[1], Changcheng Xiang[1,*], Wenjin Qin[2] and Yi Yang[3]

[1] School of Mathematics and Statistics, Hubei Minzu University, Enshi, Hubei 445000, China

[2] School of Mathematics and Computer Science, Yunnan Minzu University, Yunnan 650031, China

[3] College of Computer Science and Engineering, Chongqing Three Gorges University, Chongqing 404020, China

* **Correspondence:** Email: xcc7426681@126.com.

Abstract: In the process of spreading infectious diseases, the media accelerates the dissemination of information, and people have a deeper understanding of the disease, which will significantly change their behavior and reduce the disease transmission; it is very beneficial for people to prevent and control diseases effectively. We propose a Filippov epidemic model with nonlinear incidence to describe media's influence in the epidemic transmission process. Our proposed model extends existing models by introducing a threshold strategy to describe the effects of media coverage once the number of infected individuals exceeds a threshold. Meanwhile, we perform the stability of the equilibriua, boundary equilibrium bifurcation, and global dynamics. The system shows complex dynamical behaviors and eventually stabilizes at the equilibrium points of the subsystem or pseudo equilibrium. In addition, numerical simulation results show that choosing appropriate thresholds and control intensity can stop infectious disease outbreaks, and media coverage can reduce the burden of disease outbreaks and shorten the duration of disease eruptions.

Keywords: SIR epidemic model; media coverage; filippov system; stability

1. Introduction

With the development of human civilization, infectious diseases have emerged gradually. For instance, in the mid-14th century, the Black Death killed 25 million Europeans, or a third of the total population of Europe at the time [1]. In 2003, the SARS epidemic swept through 32 countries and regions around the world, and infected 8422 people [2, 3]. Regarding COVID-19 at the end of 2019, it took a great toll on humanity. As of August 20, 2021, according to the latest real-time statistics from the World Health Organization, the cumulative number of confirmed COVID-19 cases worldwide was approximately 200 million and the cumulative death toll was approximately 4 million [4–6].

Therefore, infectious diseases are an important research topic, that have attracted the attention of many scholars, who have been trying to establish and improve realistic mathematical models of infectious disease transmission dynamics to increase their knowledge and understanding of infectious diseases.

Based on epidemic transmission dynamics, researchers are increasingly focusing on the effect of social factors on disease transmission, such as vaccination, lifestyle, and media coverage. The impact of vaccination on disease control has been studied in the literature [7–9]. At the same time, mass media (internet, books, newspapers and others) can be effective as an important way to obtain information and deliver preventive health messages at the beginning of a disease outbreak. A large number of people can learn the disease, media coverage will have a profound psychological impact on people, which will greatly change their personal behaviors, and reduce the spread of the disease. It is very beneficial for people to actively prevent the disease and control it effectively [10, 11]. Accordingly, the establishment of mathematical models related to media coverage and in-depth research are also of great practical importance for the prevention and control of infectious diseases. The timeliness of the media impact is also a very important issue in the control of epidemics. Therefore, to further identify the potential effects of media coverage on the spread of infectious diseases, with the aid of mathematical modeling methods, we explore and analyze the predicted spread of diseases to provide a rational qualitative description of disease transmission dynamics [12–14].

The media is regarded as an important factor in disease transmission, and a great number of scholars have conducted thorough research on this issue. In 2008, Cui and Sun [12] proposed a nonlinear transmission rate as $\beta(I) = \mu e^{-mI}$, where μ is a positive number. When parameter $m = 0$, the transmission rate is linear, and when $m > 0$, this reflects the effect of media coverage on contact transmission. In 2008, Liu and Cui [13] proposed the SIR model with the transmission rate $\beta(I) = \beta_1 - \left(\frac{\beta_2}{(mI+I)}\right)$, which is a good response to the media's effect on the disease transmission process. Furthermore , the Filippov system provides a natural and reasonable framework for many realistic problems, and has been widely used in the process of various epidemics and the predator-prey relationship, particularly in controlling epidemics. When the number of infected individuals is less than a certain level, no measures are taken, and when the number of infected individuals is greater than a certain level, the media begins to report the disease. Thus, threshold strategies provide a natural description of such systems. For example, in 2012, Xiao et al., [14] proposed the SIR model with a threshold strategy using $\beta(1 - \mathrm{f})SI$ to reflect the effect of the media. In 2015, Xiao et al., [15] proposed a Filippov model with the transmission rate $\beta(I) = \exp^{-M_1(t)}\beta_0$ to reflect the impact of media coverage. Additionally, the impact of the media on infectious diseases has also been thoroughly explored [16, 17].

Based on the aforementioned research, in this study, we present a Filippov epidemic model that relies on the number of infected individuals using a threshold strategy, and include a nonlinear incidence rate. Our proposed model extends the existing model by introducing a threshold strategy to describe the effect that is revealed by media coverage once the number of infected individuals exceeds a threshold. We implement an epidemiological model using adaptive switching behavior when the number of infected individuals exceeds a threshold. We also investigate which threshold levels can be used to guide the eradication of infectious diseases.

The remainder of the paper is organized as follows: In Section 2, we develop a Filippov epidemic model with nonliner incidence. In Section 3, we examine the dynamic behaviors of two subsystems: free system S^1 and control system S^2. In Section 4, we present the sliding mode dynamics and identify the pseudo-equilibrium, and show that it exists under certain conditions and is asymptotically stable. In

Section 5, we discuss the global dynamics analysis of the Filippov system. In Section 6, we perform boundary equilibrium bifurcation analysis. In Section 7, we investigate the effect of key parameters of the Filippov system. Finally, we present the conclusion and discussion in the last section.

2. SIR model and preliminaries

2.1. Model establishment

In the classical model of infectious diseases, the transmission rate is bilinear. However, media reports, vaccination, and population density may directly or indirectly affect it, and the bilinear transmission rate function cannot adequately explain the complex phenomenon of epidemic transmission. Meanwhile, at the beginning of the disease outbreak, media can be effective as an important way to obtain information and deliver preventive health messages. A large number of people can learn about the disease that is prevalent, and simultaneously, media coverage will have a profound psychological impact on people, which will greatly change their personal behaviors, and reduce the spread and proliferation of the disease. It is very beneficial for people to actively prevent the disease and control it effectively; hence, we choose $\frac{\beta S I}{1+\alpha I^2}$ as the transmission rate. It can be used to explain the "psychological" effect and show the effect of the media.

When the number of infected individuals reaches a critical level I_0, the media makes relevant reports and people go out less to avoid being infected, which reduces the effective exposure and transmission rate. Meanwhile, the government implements control measures to reduce the spread of the disease. Based on the work in [14, 15], we classify the population into three types, that is, susceptible, infected, and recovered, and establish a SIR model with a threshold strategy. Let $S(t)$, $I(t)$ and $R(t)$ refer to the proportions of susceptible, infected, and removed individuals at the time t changes, respectively. Thus, the model is as follows:

$$\begin{cases} \frac{dS}{dt} = \Lambda - \frac{\beta S I}{1+\varepsilon\alpha I^2} - \mu S, \\ \frac{dI}{dt} = \frac{\beta S I}{1+\varepsilon\alpha I^2} - \mu I - \gamma I, \\ \frac{dR}{dt} = \gamma I - \mu R, \end{cases} \tag{2.1}$$

with

$$\varepsilon = \begin{cases} 0, & \mathrm{I} < I_0, \\ 1, & \mathrm{I} > I_0. \end{cases} \tag{2.2}$$

System (2.1) with (2.2) is a particular form of Filippov system, where a (constant) recruitment birth rate Λ is introduced in the susceptible population, β is the transmission rate, μ is the natural death rate, and γ is the recovered rate.

Because the recovered class R in system (2.1) does not affect the dynamics of the first and second equations, we only consider the first two equations of system (2.1) with (2.2) in the following, which are easily obtained as:

$$\left\{(S, I) \in R_+^2 | 0 < S + I \leq \Lambda/\mu\right\} = \Omega.$$

For $(S, I) \in \Omega$, $dS/dt|_{S=0} > 0, dI/dt|_{I=0} = 0$, and $d(S + I)/dt|_{S+I=\Lambda/\mu} < 0$. Thus, all solutions are in the Ω region; hence, Ω is an attractive domain. Let $\mathrm{H}(Z) = I - I_0$ be a function with a threshold value that depends on the number of infected individuals, and ε be a segmentation function that depends on

$I - I_0$. For convenience, let the vector $\mathrm{Z} = (S, I)^T$. Then the discontinuous switching surface Σ can be defined as

$$\Sigma = \left\{\mathrm{Z} \in \mathrm{R}_+^2 | \mathrm{H}(\mathrm{Z}) = 0\right\},$$

we call Σ the switching manifold, which is the separating boundary of the regions [18–20]. The two regions represent the free system (S^1) and the control system (S^2).

$$G_1 = \left\{Z \in R_+^2 | H(Z) < 0\right\} \quad and \quad G_2 = \left\{Z \in R_+^2 | H(Z) > 0\right\}.$$

Let

$$F_1(Z) = \begin{bmatrix} F_{11} \\ F_{12} \end{bmatrix} = \begin{bmatrix} \Lambda - \beta S I - \mu S \\ \beta S I - \mu I - \gamma I \end{bmatrix}, \tag{2.3}$$

$$F_2(Z) = \begin{bmatrix} F_{21} \\ F_{22} \end{bmatrix} = \begin{bmatrix} \Lambda - \frac{\beta S I}{1+\alpha I^2} - \mu S \\ \frac{\beta S I}{1+\alpha I^2} - \mu I - \gamma I \end{bmatrix}. \tag{2.4}$$

Hence, system (2.1) can be rewritten as the Filippov system using the following form:

$$\dot{Z} = \begin{cases} F_1(Z), & Z \in G_1, \\ F_2(Z), & Z \in G_2. \end{cases} \tag{2.5}$$

For convenience, we present the following definitions of all the types of equilibria of the Filippov system [21, 22].

Definition 2.1. *If the equilibrium point Z^* of the sliding line region Σ_s of system 2.1 satisfies $\lambda F_1(Z^*) + (1-\lambda) F_2(Z^*) = 0, H(Z^*) = 0$ with $0 < \lambda < 1$, where*

$$\lambda = \frac{\langle H_Z(Z^*), F_2(Z^*)\rangle}{\langle H_Z(Z^*), F_2(Z^*) - F_1(Z^*)\rangle},$$

then Z^* is called the pseudo-equilibrium point of the system.

Definition 2.2. *If $Z \in G_1$ and $F_1(Z) = 0$ or $Z \in G_2$ and $F_2(Z) = 0$, then Z is the real equilibrium point of system 2.1. If $Z \in G_1$ and $F_2(Z) = 0$ or $Z \in G_2$ and $F_1(Z) = 0$, then Z is the virtual equilibrium point of system 2.1.*

Definition 2.3. *If $Z \in \Sigma$ and $F_1(Z) = 0$ or $F_2(Z) = 0$, then Z is called the boundary point of system 2.1.*

Moreover, if $F_i(Z) = 0$ is invertible, we say that a boundary equilibrium bifurcation occurs at Z. These bifurcations are classified as the boundary focus bifurcation and boundary node bifurcation in [23–25].

Definition 2.4. *If $Z \in \Sigma$ and $HF_1(Z) = 0$ or $HF_2(Z) = 0$, then Z is called the tangent point of system 2.1.*

3. Dynamics analysis of subsystems

Before analyzing the complete switching system, it is first necessary to determine the dynamical behaviors of the two subsystems. According to the method in [26, 27], the basic reproduction number is considered as $R_0 = \frac{\beta\Lambda}{(\mu+\gamma)\mu}$ in system S^1. Meanwhile, according to this equation $\mu\alpha(\mu+\gamma)\mathrm{I}^2 + (\mu+\gamma)\beta I + \mu(\mu+\gamma) - \Lambda\beta = 0$, we obtain the basic reproduction number $R_c = \frac{\beta\Lambda}{(\mu+\gamma)\mu}$ in system S^2. Therefore, it is obvious that $R_0 = R_c = \frac{\beta\Lambda}{(\mu+\gamma)\mu}$.

3.1. Dynamics for the free system S^1

In this section, we analyze the stability of the equilibrium point in the free system and define a suitable Lyapunov function to verify the global stability. The free system has two equilibrium points: disease-free equilibrium and endemic equilibrium. The disease-free equilibrium point is $E_0 = \left(\frac{\Lambda}{\mu}, 0\right)$ and the endemic equilibrium point is $E_1 = \left(\frac{\mu+\gamma}{\beta}, \frac{\Lambda\beta-(\mu^2+\mu\gamma)}{\beta(\mu+\gamma)}\right)$.

Lemma 1. The disease-free equilibrium point $E_0 = \left(\frac{\Lambda}{\mu}, 0\right)$ in system S^1 is globally asymptotically stable if $R_0 < 1$ and unstable if $R_0 > 1$, whereas the endemic equilibrium point $E_1 = (S_1, I_1)$ is globally asymptotically stable if $R_0 > 1$.

3.2. Dynamics for the control system S^2

For the control system S^2, the disease-free equilibrium point is easily obtained as $E_2 = E_0 = \left(\frac{\Lambda}{\mu}, 0\right)$ and the endemic equilibrium point is the solution of the following algebraic equation:

$$\begin{cases} \Lambda - \frac{\beta S I}{1+\alpha I^2} - \mu S = 0, \\ \frac{\beta S I}{1+\alpha I^2} - \mu I - \gamma I = 0, \end{cases}$$

the equation for I is obtained as

$$A\mathrm{I}^2 + BI + C = 0,$$

where

$$A = \mu\alpha(\mu+\gamma),$$
$$B = (\mu+\gamma)\beta,$$
$$C = \mu(\mu+\gamma)[1-R_0].$$

Then, we can solve the equation with respect to I to obtain

$$I_i = \frac{-B \pm \sqrt{\Delta}}{2A} (i = 3, 4),$$

where

$$\Delta = (\mu\beta + \gamma\beta)^2 - 4\alpha\left(\mu\gamma + \mu^2\right)^2 [1 - R_0].$$

Because parameters $\mu, \alpha, \beta, \gamma$ are non-negative, $A > 0$ and $B > 0$. When $C < 0$, that is, $R_0 > 1$, a unique positive solution

$$I_3 = \frac{-B + \sqrt{\Delta}}{2A} > 0$$

exists; hence, we have the following summary:

i) If $R_0 < 1$, then no positive equilibrium exists.

ii) If $R_0 > 1$, then a unique positive equilibrium $E_3 = (S_3, I_3)$ exists, which is called the endemic equilibrium and given by

$$\mathrm{S}_3 = \frac{(\mu+\gamma)\left(1+\alpha\mathrm{I}_3^2\right)}{\beta},$$

$$\mathrm{I}_3 = \frac{-(\mu\beta+\gamma\beta) + \sqrt{\Delta}}{2\mu\alpha(\mu+\gamma)}.$$

Lemma 2. If $R_0 < 1$, then the disease-free equilibrium point E_2 in the system S^2 is globally asymptotically stable.

Theorem 1. If $R_0 > 1$, then the endemic equilibrium point E_3 is locally asymptotically stable.

proof. The Jacobian matrix of the control system S^2 at E_3 is

$$M = \begin{pmatrix} \frac{-\beta I_3}{1+\alpha I_3^2} - \mu & \frac{-\beta S_3}{1+\alpha I_3^2} + \frac{2\alpha\beta S_3 I_3^2}{\left(1+\alpha I_3^2\right)^2} \\ \frac{\beta I_3}{1+\alpha I_3^2} & \frac{\beta S_3}{1+\alpha I_3^2} - \frac{2\alpha\beta S_3 I_3^2}{\left(1+\alpha I_3^2\right)^2} - \mu - \gamma \end{pmatrix},$$

the characteristic equation, for this matrix, becomes

$$\lambda^2 - \mathrm{tr}\,(M)\,\lambda + \det(M) = 0,$$

where

$$\det(M) = \left(\frac{\beta I_3}{1+\alpha I_3^2} + \mu\right)(\mu+\gamma) + \frac{\mu\beta S_3\left(\alpha I_3^2 - 1\right)}{\left(1+\alpha I_3^2\right)^2},$$

$$\mathrm{tr}\,(M) = \frac{-\beta I_3}{1+\alpha I_3^2} - 2\mu + \frac{\beta S_3}{1+\alpha I_3^2} - \frac{2\alpha\beta S_3 I_3^2}{\left(1+\alpha I_3^2\right)^2} - \gamma.$$

If $det(M) > 0$, $tr(M) < 0$, that is, $R_0 > 1$, then the endemic equilibrium point E_3 is a stable focus or node.

4. Sliding mode and its dynamics

In this section, we consider the sliding mode and its dynamics. First, we review the definition of the sliding mode segment, calculate the pseudo-equilibrium point, and provide sufficient conditions for the existence of the pseudo-equilibrium point. In mathematics, there are two approaches to determine sufficient conditions for the appearance of sliding mode on discontinuous surfaces: the Filippov convex method [28] and Utkin's equivalent control method [29]. Then, according to Definition 2.1, we determine the existence of the sliding mode domain of system 2.1.

Let

$$\sigma(Z) = \langle H_Z(Z), F_1(Z)\rangle \langle H_Z(Z), F_2(Z)\rangle,$$

where $\langle\cdot,\cdot\rangle$ denotes the standard scalar product and $H_Z(Z)$ is the invariant gradient of the smooth scalar function $H(Z)$ in Σ. The sliding domain is defined as $\Sigma_s = \{Z \in \Sigma | \sigma(Z) < 0\}$, and $H(I) = I - I_0$, which means that $H_Z(Z) = (0,1)^T$. Since $F_1(Z) = (F_{11}(Z), F_{12}(Z))^T$, $F_2(Z) = (F_{21}(Z), F_{22}(Z))^T$. For more information about the Filippov system, readers can refer to [30–32].

When

$$\sigma(Z) = \langle H_Z(Z), F_1(Z)\rangle \langle H_Z(Z), F_2(Z)\rangle = F_{12}(Z)\,F_{22}(Z) \le 0,$$

then it's obvious that $F_{12}(Z) > F_{22}(Z)$. Hence, we obtain

$$\Sigma_s = \{(S,I) \in \Sigma | F_{12}(S,I) \ge 0, F_{22}(S,I) \le 0\}.$$

Let the endpoints of the slide segment be $A(S_L, I_0), B(S_R, I_0)$, where $S_L = \frac{\mu+\gamma}{\beta}$, $S_R = \frac{(\mu+\gamma)\left(1+\alpha I_0^2\right)}{\beta}$; hence, the sliding domain of the Filippov system is as follows:

$$\Sigma_s = \left\{(S, I) \in R_+^2 | S_L \leq S \leq S_R, I = I_0\right\}.$$

Assuming that the second equation of the system (2.1) is equal to 0, we obtain $\frac{\beta S I}{1+\varepsilon\alpha I^2} = \mu I + \gamma I$. Substituting $I = I_0$ and $\frac{\beta S I}{1+\varepsilon\alpha I^2} = \mu I + \gamma I$ into the first equation of system (2.1), we obtain

$$\frac{dS}{dt} = \Lambda - \mu I_0 - \mu S - \gamma I_0 = f(S).$$

Let $f(S) = 0$. Thus, we obtain

$$S_p = \frac{\Lambda - \mu I_0 - \gamma I_0}{\mu},$$

therefore, the coordinates of the possible pseudo-equilibrium point are given by $E_p = \left(S_p, I_0\right)$.

When

$$S_p - S_L = \frac{\Lambda - \mu I_0 - \gamma I_0}{\mu} - \frac{(\mu+\gamma)}{\beta} = \frac{\Lambda\beta - (\mu+\gamma)\beta I_0 - \mu(\mu+\gamma)}{\mu\beta} > 0,$$

$$S_p - S_R = \frac{\Lambda - \mu I_0 - \gamma I_0}{\mu} - \frac{(\mu+\gamma)\left(1+\alpha I_0^2\right)}{\beta} = \frac{\Lambda\beta - (\mu+\gamma)\beta I_0 - \mu(\mu+\gamma)\left(1+\alpha I_0^2\right)}{\mu\beta} < 0,$$

(i.e., $(\mu+\gamma)(\beta I_0 + \mu) < \Lambda\beta < (\mu+\gamma)\left[\beta I_0 + \mu\left(1+\alpha I^2\right)\right]$). Thus, when $S_L \leq S_p \leq S_R$, the pseudo-equilibrium point E_p is in sliding mode. Additionally, because $f\left(S_p\right)' \leq 0$, the pseudo-equilibrium point E_p is locally asymptotically stable. When $S_p > S_R$ or $S_p < S_L$, the pseudo-equilibrium point E_p is not in the sliding mode.

To analyze the relationship between the sliding domain and the attraction domain, we solve the following equation:

$$\frac{\mu+\gamma}{\beta} = \frac{\Lambda}{\mu} - I \quad and \quad \frac{(\mu+\gamma)\left(1+\alpha I^2\right)}{\beta} = \frac{\Lambda}{\mu} - I.$$

It is easy to derive

$$I_0^1 = \frac{\Lambda}{\mu} - \frac{\mu+\gamma}{\beta}, \qquad I_0^3 = \frac{-\mu\beta + \sqrt{\Delta}}{2\mu\alpha(\mu+\gamma)},$$

where

$$\Delta = (\mu\beta)^2 - 4\mu\alpha(\mu+\gamma)\left[\mu(\mu+\gamma) - \Lambda\beta\right].$$

Regarding the bifurcation set phase diagram of the control intensity $\alpha - I_0$ shown in Figure 1, we obtain the following: If $I_0 < I_3$ (i.e., region Γ^1 in Figure 1), the equilibrium point E_1 of the free system S^1 is virtual, which is denoted by E_1^V, and the equilibrium point E_3 of the control system S^2 is real, which is denoted by E_3^R. If $I_3 < I_0 < I_1$ (i.e., region $\Gamma^2 \cup \Gamma^3$ in Figure 1), the endemic equilibria E_1 and E_3 of both system S^1 and system S^2 are virtual, which are denoted by E_1^V and E_3^V, respectively. At this moment, E_1^V, E_3^V, and E_p coexist. When $I_1 < I_0$ (i.e., region $\Gamma^4 \cup \Gamma^5 \cup \Gamma^6$ in Figure 1), the endemic equilibrium point E_1 of the free system S^1 is real, which is denoted by E_1^R. The endemic equilibrium point E_3 of the control system S^2 is virtual, which is denoted by E_3^V (see Definition 2.2 for details).

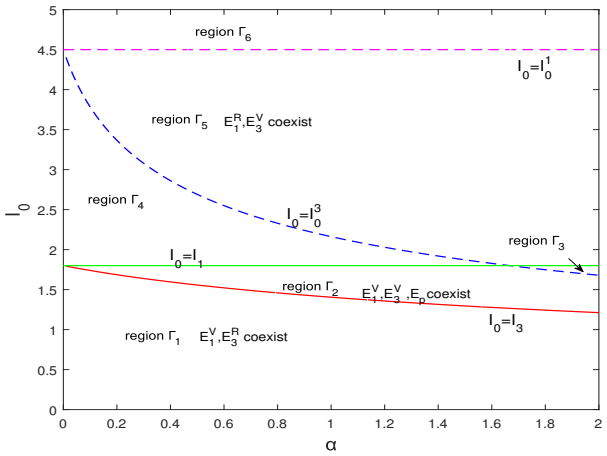

Figure 1. System 2.1 with 2.2 on the branching set of the control intensity α and the threshold I_0. Let Γ_1 be the domain bounded by $\alpha = 0$, $\alpha = 2$, $I_0 = 0$ and the curve $I_0 = I_3$; Γ_2 is the domain bounded by $\alpha = 2$, $I_0 = I_1$, the curve $I_0 = I_0^3$ and the curve $I_0 = I_3$; Γ_3 be the domain bounded by $\alpha = 2$, $I_0 = I_1$ and the curve $I_0 = I_0^3$; Γ_4 be the domain bounded by $\alpha = 0$, $I_0 = I_1$ and the curve $I_0 = I_0^3$; Γ_5 is the domain bounded by $\alpha = 2$, $I_0 = I_1$, $I_0 = I_0^1$ and the curve $I_0 = I_0^3$; Γ_6 is the domain bounded by $\alpha = 0$, $\alpha = 2$, $I_0 = I_0^1$ and $I_0 = 5$, which we fix the other parameters as $\Lambda = 1$; $\beta = 1$; $\mu = 0.2$; $\gamma = 0.3$.

5. Global behavior of the Filippov system

In the previous section, we studied the regular equilibrium, virtual equilibrium, and pseudo-equilibrium. The pseudo-equilibrium point exists and is locally asymptotically stable under certain conditions. In this section, we discuss the dynamical behaviors of the Filippov system 2.1 with 2.2. We adjust the parameters and find that the system changed from stable to unstable because of the change of parameter β. The phase portrait of system 2.1 shows that S and I eventually tended to a stable value as time t changed, as shown in Figure 2. The time response of the states of system 2.1 for different initial values is shown in Figure 3(a),(b). The S-I phase portrait presents the periodic solution, as shown in Figure 3(c).

Next, we specifically describe the branching phase diagram in (Figure 1). If $R_0 < 1$, the disease is eradicated; hence, we only consider the dynamical behaviors of the system if $R_0 > 1$.

1) If $I_0 < I_3$ (region Γ^1), the endemic equilibrium point E_1 is virtual in the free system S^1, which is denoted by E_1^V, and the endemic equilibrium point E_3 in the control system S^2 is real , which is denoted by E_3^R. The trajectories of different initial values eventually converge to the real equilibrium E_3^R, as shown in Figure 4(a),(b).

2) If $I_3 < I_0 < I_1$ (region $\Gamma^2 \cup \Gamma^3$), the endemic equilibrium points E_1 and E_3 in the free system and control system are virtual denoted by E_1^V and E_3^V, respectively. In this case , the pseudo-equilibrium point exists and is locally asymptotically stable, as shown in Figure 4(c). The trajectories of different initial values eventually converge to the pseudo-equilibrium point E_p, as shown in Figure 4(c),(d).

3) If $I_1 < I_0$ (region $\Gamma^4 \cup \Gamma^5 \cup \Gamma^6$), the endemic equilibrium point E_1 of the free system S^1 is the real equilibrium point, which is denoted by E_1^R, and the endemic equilibrium point E_3 of the control system S^2 is the virtual equilibrium point, which is denoted by E_3^V. The trajectories of different initial values

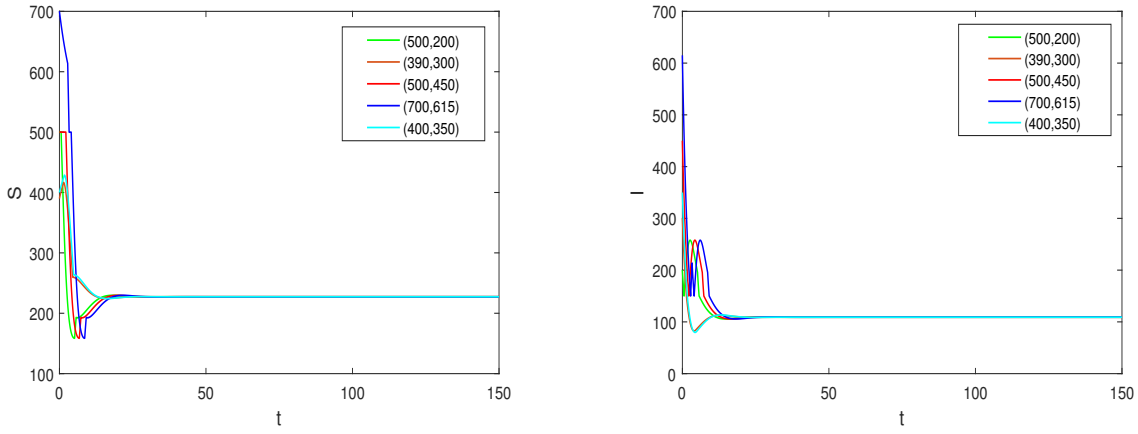

(a) (b)

Figure 2. The parameters values are $\Lambda = 100$; $\beta = 0.0022$; $\mu = 0.2$;$\alpha = 0.3$; $\gamma = 0.3$, at the moment, the system is stable.

eventually converge to the real equilibrium E_1^R, as shown in Figure 4(e),(f).

To obtain the richer dynamical behaviors that the system may exhibit, we chose the parameters $\alpha = 0.6$ and $\gamma = 0.1$, and all other parameters remained unchanged. The corresponding simulations are shown in Figure 5.

In Figure 5, for different initial values, our main results show that the system eventually stabilizes at the equilibrium points E_1 and E_3, or the pseudo-equilibrium E_p, which is strongly related to the threshold value I_0. In particular, when we choose a sufficiently small threshold level I_0 (i.e., $I_0 < I_3$), the control policy is always triggered; hence, the solution of the system eventually tends to the endemic equilibrium or disease-free equilibrium (not labeled in the Figure), as shown in Figure 5(a),(b). Then, we choose the threshold I_0 as an intermediate value (i.e., $I_3 < I_0 < I_1$), the trajectories of different initial values eventually converge to the pseudo-equilibrium point E_p, as shown in Figure 5(c). When we choose a sufficiently large threshold level I_0 (i.e., $I_0 > I_1$), the control strategy is not triggered, and the solution converges to the endemic equilibrium E_1^R of the subsystem at this moment, which depends on the individual parameter values, as shown in Figure 5(d). Clearly, the trajectories are influenced by the isoclines and the switching line in Figures 4 and 5.

6. Boundary equilibrium bifurcation analysis

To demonstrate the boundary equilibrium bifurcation of system 2.1, we choose I_0 as the bifurcation parameter and fix the other parameters. The definitions of the boundary equilibrium point and tangent point are shown in the Definitions 2.3 and 2.4, respectively. The equations satisfied by the boundary equilibrium of system 2.1 are as follows:

$$\wedge - \frac{\beta S I}{1 + \epsilon\alpha I^2} - \mu S = 0, \quad \frac{\beta S I}{1 + \epsilon\alpha I^2} - \mu I - \gamma I = 0, \quad I = I_0.$$

To ensure that the boundary equilibrium point exists, for both $\epsilon = 0$ and $\epsilon = 1$, it is necessary to

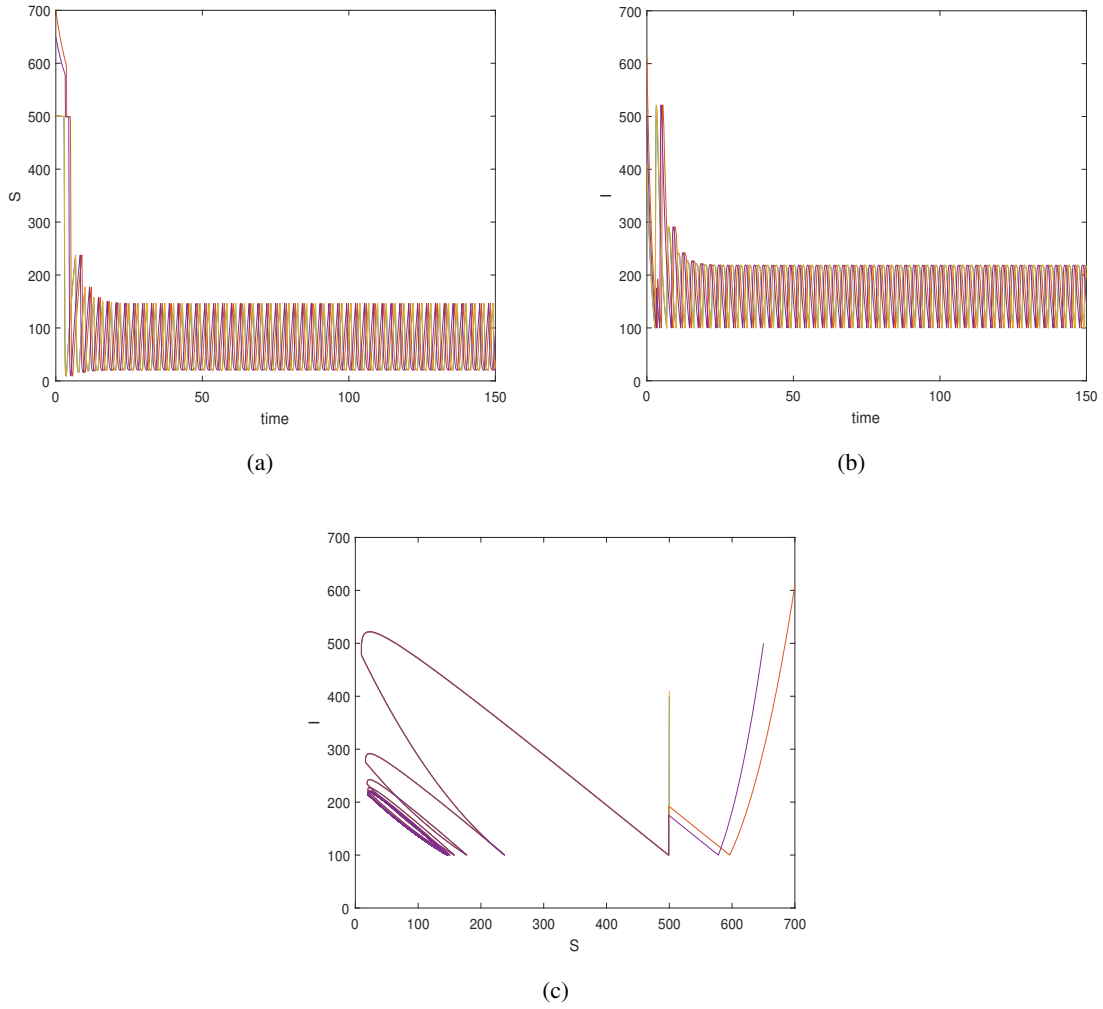

(a) (b)

(c)

Figure 3. (a) and (b) represents the phase diagram of S, I as time t, (c) represents the S-I phase diagram. In (a) and (b), the parameters are $\Lambda = 100$, $\beta = 0.022$, $\mu = 0.2$, $\alpha = 0.3$, $\gamma = 0.3$, while the system 2.1 is unstable and forms a periodic solution.

satisfy

$$\frac{\Lambda\left(1+\epsilon\alpha I_0^2\right)}{\beta I_0+\mu\left(1+\epsilon\alpha I_0^2\right)}=\frac{(\mu+\gamma)\left(1+\epsilon\alpha I_0^2\right)}{\beta},$$

which indicates that $I_0 = I_1$ ($I_0 = I_3$) for $\epsilon = 0$ ($\epsilon = 1$). Thus, there are four possible boundary equilibria:

$$E_b^{11}=\left(\frac{\Lambda}{\beta I_1+\mu},I_1\right),\quad E_b^{21}=\left(\frac{\Lambda\left(1+\alpha I_1^2\right)}{\beta I_1+\mu\left(1+\alpha I_1^2\right)},I_1\right),$$

$$E_b^{12}=\left(\frac{\Lambda}{\beta I_3+\mu},I_3\right),\quad E_b^{22}=\left(\frac{\Lambda\left(1+\alpha I_3^2\right)}{\beta I_3+\mu\left(1+\alpha I_3^2\right)},I_3\right).$$

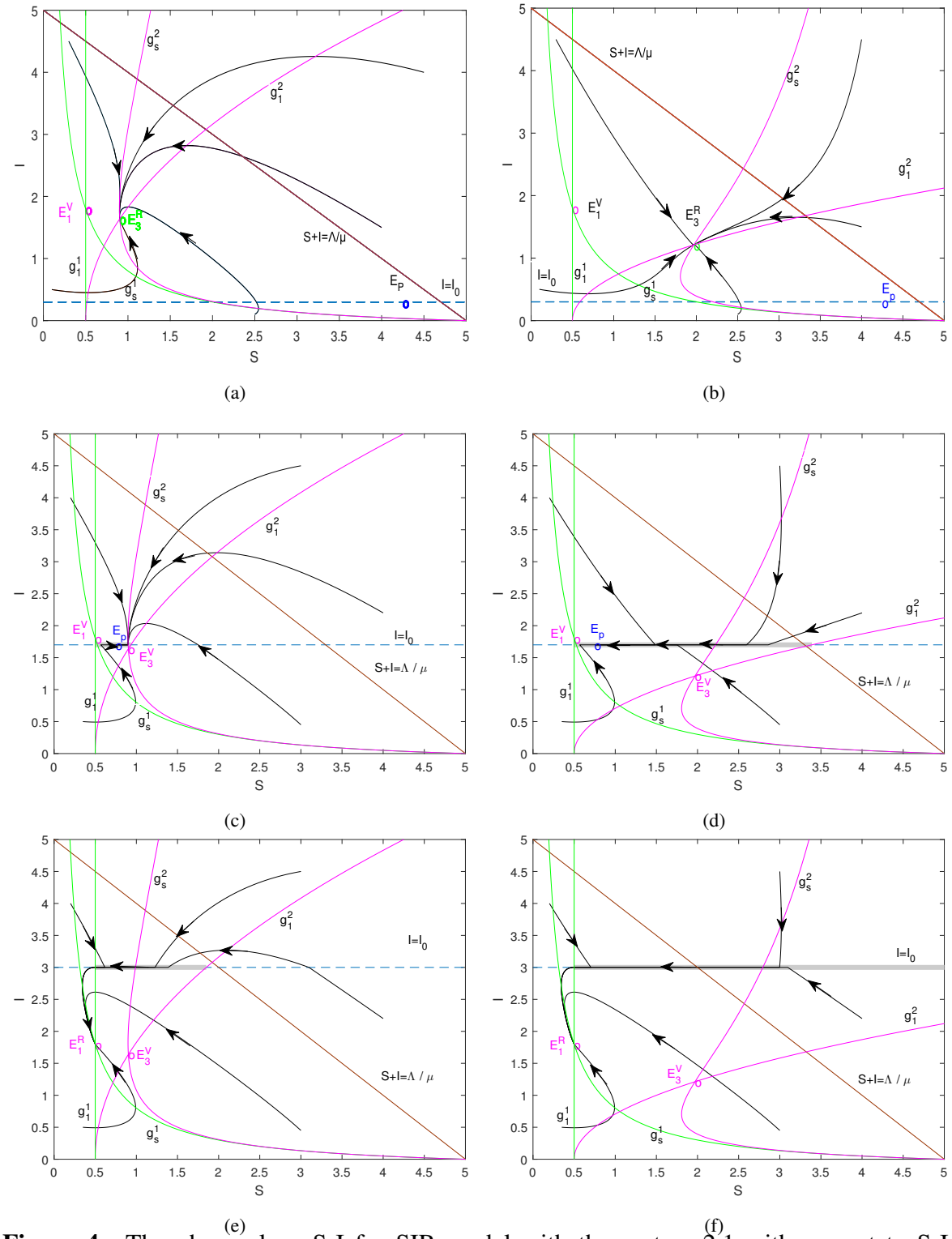

Figure 4. The phase plane S-I for SIR model with the system 2.1 with respect to S-I, showing the behaviors of the solution for different parameters and thresholds. The isoclinic lines(green) g_1^1 (g_s^1) and (pink) g_1^2 (g_s^2) are plotted for the free (control) system $S^1(S^2)$. Parameters values are $\Lambda = 1$; $\beta = 1$; $\mu = 0.2$; $\gamma = 0.3$, where the control intensity and thresholds are (a) $\alpha = 0.3$,$I_0 = 0.3$, (c) $\alpha = 0.3$, $I_0 = 1.7$, (e) $\alpha = 0.3$, $I_0 = 3$. (b)$\alpha = 2$, $I_0 = 0.3$, (d)$\alpha = 2$, $I_0 = 1.7$, (f) $\alpha = 2$, $I_0 = 3$, different kinetic behaviors are also obtained.

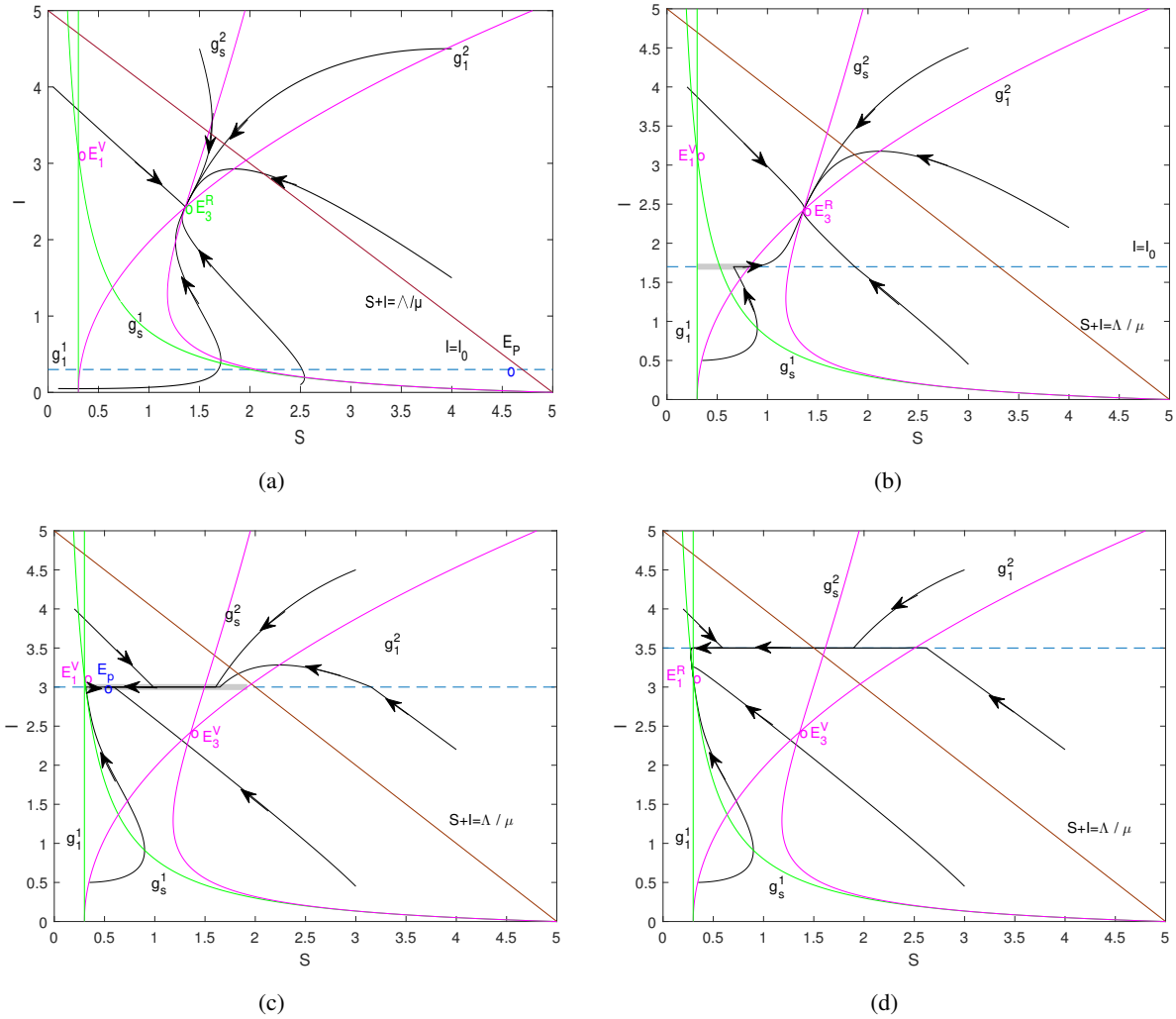

Figure 5. The phase plane S-I for SIR model with the system 2.1. The isoclinic lines (green) g_1^1 (g_s^1) and (pink) g_1^2 (g_s^2) are plotted for the free (control) system $S^1(S^2)$. Parameters values are $\Lambda = 1$; $\beta = 1$; $\mu = 0.2$; $\alpha = 0.6$; $\gamma = 0.1$, where the thresholds are (a) $I_0 = 0.3$, (b) $I_0 = 1.7$, (c) $I_0 = 3$, (d) $I_0 = 3.5$.

The equation satisfied by the tangent point is as follows:

$$\frac{\beta S I}{1+\epsilon\alpha I^2} - \mu I - \gamma I = 0, \quad \mathrm{I} = \mathrm{I}_0,$$

by solving the above equation, we obtain the tangent point as

$$\mathrm{T}_1 = \left(\frac{\mu+\gamma}{\beta}, I_0\right), \quad \mathrm{T}_2 = \left(\frac{(\mu+\gamma)\left(1+\alpha I_0^2\right)}{\beta}, I_0\right).$$

When the threshold value I_0 passes a certain critical value, a boundary equilibrium bifurcation may occur if the real equilibrium, tangent point, and pseudo-equilibrium (or tangent point and real equilibrium) collide [14, 23, 30]. When the threshold value I_0 passes the first critical value $I_0 = I_3$, the equilibrium E_3^R, pseudo-equilibrium point E_p, and tangent point T_2 collide, which is denoted by E_B^1, as shown in Figure 6, where $I_0 = 1.2122$. In this case, the boundary equilibrium E_B^1 is an attractor. When the threshold value I_0 passes the second critical value $I_0 = I_1$, the equilibrium E_1^R, pseudo-equilibrium point E_p, and tangent point T_1 collide, which is denoted by E_B^2, where $I_0 = 1.8$. In this case, the boundary equilibrium E_B^1 is an attractor. Overall, there are two boundary equilibrium bifurcations in Figure 6.

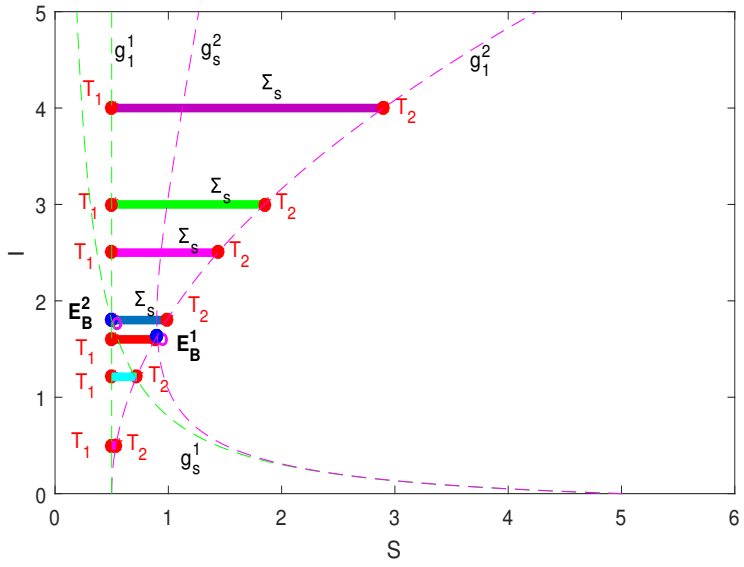

Figure 6. Boundary equilibrium bifurcations for system 2.1. The isoclinic lines (green) g_1^1 (g_s^1) and (pink) g_1^2 (g_s^2) are plotted for the free (control) system $S^1(S^2)$. The parameter values are $\Lambda = 1$; $\beta = 1$; $\mu = 0.2$; $\alpha = 0.3$; $\gamma = 0.3$, where the thresholds are $I_0 = 0.5$, $I_0 = 1.2122$, $I_0 = 1.6$, $I_0 = 1.8$, $I_0 = 2.5$, $I_0 = 3$, $I_0 = 4$, respectively.

7. The effect of the key parameters of the Filippov system

For system 2.1, our aim is to find an effective strategy to adjust the infected population below a certain value or to be eliminated. It is important to implement the control strategy by setting an

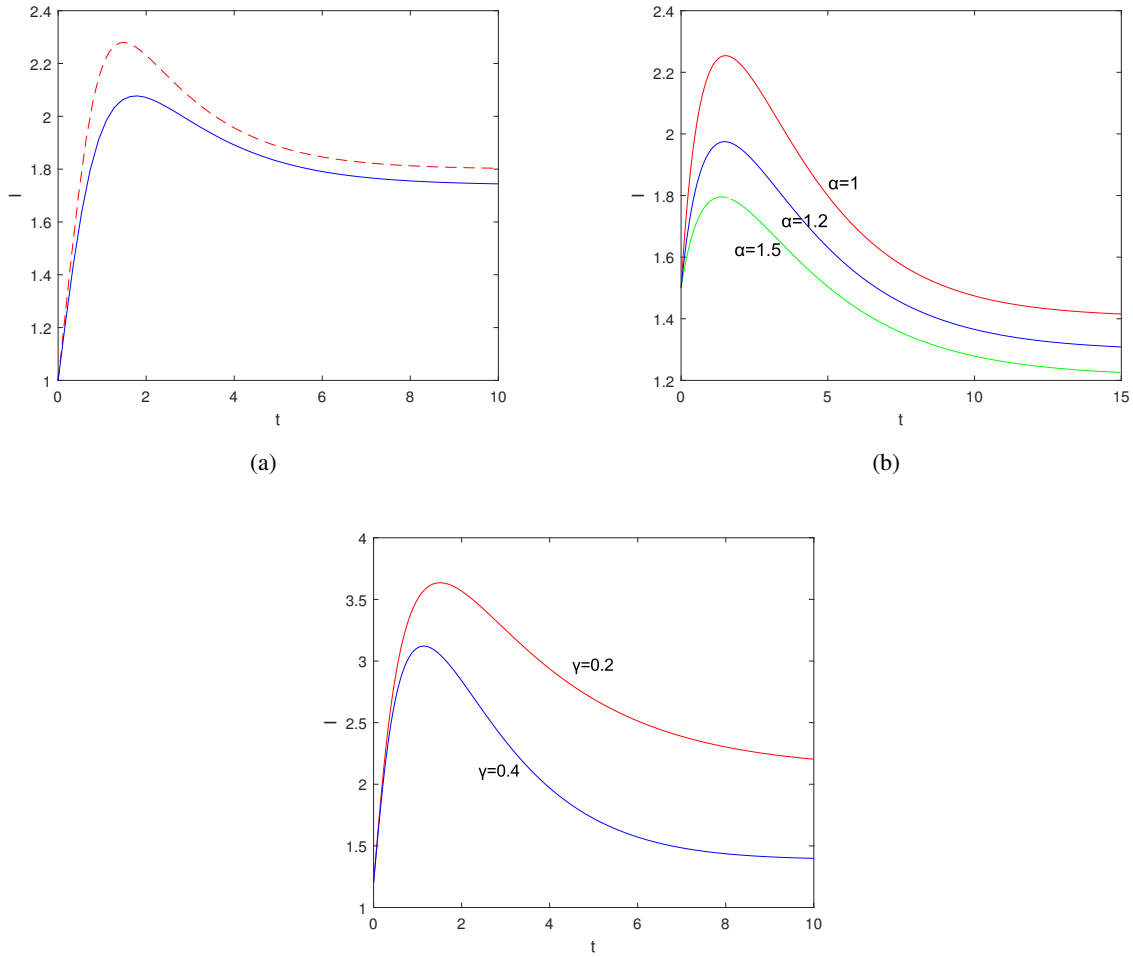

(a) (b)

(c)

Figure 7. The dynamic behaviors of infected in system 2.1 within time. Parameters values are (a) $\Lambda = 1$; $\beta = 1$; $\mu = 0.2$; $\alpha = 0.2$; $\gamma = 0.3$. In (b) and (c), all other parameters are the same as shown in (a), except α and γ, which are illustrated in each subfigure.

appropriate threshold I_0. We choose control intensity α and recovery rate γ as key parameters and study how these parameters affect the dynamics of the system.

The red dashed line represents the free system and the blue solid line represents the control system affected by the media coverage. From Figure 7(a), it can be obtained that the media coverage makes the peak lower and delays the appearance of the peak. In Figure 7(b), we find that the peak reduces as the control intensity α increases. A similar trend appears in Figure 7(c), which means that media coverage and recovery treatment can be helpful in controlling infectious diseases.

8. Conclusions and discussion

In early epidemic models, incidence rates were bilinear, but bilinear incidence rates cannot explain the spread of epidemics very well under realistic conditions. Meanwhile, the Filippov system provides a natural and reasonable framework for many realistic problems and has been widely used in the process of various epidemics and the predator-prey relationship, particularly in controlling epidemics. Accordingly, we proposed a Filippov epidemic model with nonlinear incidence to describe the influence of the media on the epidemic transmission process. Our proposed model extends existing models by introducing a threshold strategy to describe the media effects.

When the number of infected individuals reaches or exceeds threshold I_0, another adaptive system with a nonlinear incidence rate is used, at which time the disease is widely reported immediately and people become aware of the disease, and thus take certain protective measures to reduce the possibility of being infected. Thus, the number of new infections per day is reduced to a certain level. This shows that the typical threshold behavior is completely valid. First, we analyzed the stability of each equilibrium in system 2.1. Then, we used the theory of the Filippov system [28, 31, 32] to discuss the existence of sliding regions, the pseudo-equilibrium, and the real and virtual properties of each equilibrium of the system. Next, we studied the global stability of system 2.1 and boundary equilibrium bifurcation. Finally, we obtained biological conclusions from the theoretical and numerical simulation results of the system.

Our main results showed that the system eventually stabilized at the equilibrium points E_1 or E_3 or the pseudo-equilibrium E_p, which was strongly related to the threshold value I_0. Meanwhile, our findings indicate that by setting the appropriate threshold I_0, the relevant health authorities can decide whether to intervene to effectively control the disease at a relatively low level. Simultaneously, the media's real-time coverage of the disease has had a psychological impact on humans that leads them to change their behavior, which results in a decrease in the number of infections. In Figure 7, we find that media coverage decreases the peak of the disease outbreak and delays its occurrence. Meanwhile, to a certain extent, the peak of the disease outbreak decreases with the increase of media coverage. This implies that media coverage is effective in controlling infectious diseases. We further demonstrated that media coverage is important for disease prevention and control.

Although we determined meaningful implications for disease control in this study, it still has some drawbacks. For example, we only considered the relationship between the number of infected individuals and a certain threshold to construct the switching condition. Actual disease-control strategies depend on more than the number of infected individuals. We did not take rapid growth rates into account, and this will be our next step in future work.

Acknowledgments

This work was supported by The National Natural Science Foundation of China (Grant No.11961024).

Conflict of interest

The authors declare no conflict of interest.

References

1. K. I. Bos, V. J. Schuenemann, G. B. Golding, A draft genome of yersinia pestis from victims of the black death, *Nature*, **478** (2011), 506–510. https://doi.org/10.1038/nature10549
2. Z. B. Zhang, The outbreak pattern of SARS cases in China as revealed by a mathematical model, *Ecol. Model.*, **204** (2007), 420–426. https://doi.org/10.1016/j.ecolmodel.2007.01.020
3. L. Hailong, R. X. Yu, L. Shuang, Analysis of the efficiency of the preventing and isolating treatments of SARS based on mathematical model, *Int. J. Biomath.*, **19** (2004), 72–76. https://doi.org/10.2116/analsci.20.717
4. X. S. Zhang, E. Vynnycky, A. Charlett, Transmission dynamics and control measures of COVID-19 outbreak in China: a modelling study, *Sci. Rep.*, **11** (2021), 1–12. https://doi.org/10.1038/s41598-021-81985-z
5. J. W. Deng, S. Y. Tang, H. Y. Shu, Joint impacts of media, vaccination and treatment on an epidemic Filippov model with application to COVID-19, *J. Theor. Biol.*, **523** (2021), 110698. https://doi.org/10.1016/j.jtbi.2021.110698
6. S. He, S. Y. Tang, L. B. Rong, A discrete stochastic model of the COVID-19 outbreak: forecast and control, *Math. Biosci. Eng.*, **17** (2020), 2792–2804. https://doi.org/10.3934/mbe.2020153
7. A. Ibeas, M. D. L. Sen, S. A. Quesada, Robust sliding control of SEIR epidemic models, *Math. Biosci. Eng.*, **2014** (2014), 11. https://doi.org/10.1155/2014/104764
8. M. Sharifi, H. Moradi, Nonlinear robust adaptive sliding mode control of influenza epidemic in the presence of uncertainty, *J. Process. Contr.*, **56** (2017), 48–57. https://doi.org/10.1016/j.jprocont.2017.05.010
9. A. Wang, Y. Xiao, Sliding bifurcation and global dynamics of a filippov epidemic model with vaccination, *Int. J. Bifurcat. Chaos*, **23** (2013), 1350144. https://doi.org/10.1142/S0218127413501447
10. J. M. Tchuenche, N. Dube, C. P. Bhunu, R. J. Smith, C. T. Bauch, The impact of media coverage on the transmission dynamics of human influenza, *BMC Public Health*, **11** (2011), 1–16. https://doi.org/10.1186/1471-2458-11-S1-S5
11. J. M. Tchuenche, C. T. Bauch, Dynamics of an infectious disease where media coverage influences transmission, *Int. Schol. Res. Not.*, **2012** (2012), 1–10. https://doi.org/10.5402/2012/581274

12. J. G. Cui, Y. H. Sun, H. P. Zhu, The impact of media on the control of infectious diseases, *J. Dyn. Differ. Equations*, **20** (2008), 31–53. https://doi.org/10.1007/s10884-007-9075-0
13. Y. Liu, J. A. Cui, The impact of media coverage on the dynamics of infectious disease, *Int. J. Biomath.*, **1** (2008), 65–74. https://doi.org/10.1142/S1793524508000023
14. Y. N. Xiao, X. X. Xu, S. Y. Tang, Sliding mode control of outbreaks of emerging infectious diseases, *B. Math. Biol.*, **74** (2012), 2403–2422. https://doi.org/10.1007/s11538-012-9758-5
15. Y. N. Xiao, S. Y. Tang, J. H. Wu, Media impact switching surface during an infectious disease outbreak, *Sci. Rep.*, **5** (2015), 1–9. https://doi.org/10.1038/srep07838
16. Y. H. Zhang, Y. N. Xiao, Global dynamics for a filippov epidemic system with imperfect vaccination, *Nonlinear Anal. Hybri.*, **38** (2020), 100932. https://doi.org/10.1016/j.nahs.2020.100932
17. Y. H. Zhang, P. F. Song, Dynamics of the piecewise smooth epidemic model with nonlinear incidence, *Chaos Soliton. Fract.*, **146** (2020), 110903. https://doi.org/10.1016/j.chaos.2021.110903
18. Y. Yang, X. F. Liao, Filippov hindmarsh-rose neuronal model with threshold policy control, *IEEE T. Neur. Net. Lear.*, **30** (2019), 306–311. https://doi.org/10.1109/TNNLS.2018.2836386
19. T. Carvalho, L. F. Gonçalves, Combing the hairy ball using a vector field without equilibria, *J. Dyn. Control Syst.*, **26** (2020), 233–242. https://doi.org/10.1007/s10883-019-09446-5
20. D. C. Vicentin, P. F. A. Mancera, T. Carvalho, Mathematical model of an antiretroviral therapy to HIV via Filippov theory, *Appl. Math. Comput.*, **387** (2020), 125179. https://doi.10.1016/j.amc.2020.125179
21. M. D. Bernardo, C. J. Budd, A. R. Champneys, P. Kowalczyk, Bifurcations in nonsmooth dynamical systems, *Siam. Rev.*, **50** (2008), 629–701. https://doi.10.1137/050625060
22. M. Guardia, T. M. Seara, M. A. Teixeira, Generic bifurcations of low codimension of planar filippov systems, *J. Differ. Equations*, **250** (2011), 1967–2023. https://doi.10.1016/j.jde.2010.11.016
23. W. Qin, S. Tang, The selection pressures induced non-smooth infectious disease model and bifurcation analysis, *Chaos Solition. Fract.*, **69** (2014), 160–171. https://doi.10.1016/j.chaos.2014.09.014
24. A. Wang, Y. Xiao, R. A. Cheke, Global dynamics of a piece-wise epidemic model with switching vaccination strategy, *Discrete. Cont. Dyn.-B.*, **19** (2014), 2915–2940. https://doi.10.3934/dcdsb.2014.19.2915
25. S. Tang, Y. Xiao, N. Wang, H. Wu, Piecewise HIV virus dynamic model with CD4(+) T cell count-guided therapy: I, *J. Theor. Biol.*, **308** (2012), 123–134. https://doi.org/10.1016/j.jtbi.2012.05.022
26. P. V. D. Driessche, J. Watmough, Reproduction numbers and sub-threshold endemic equilibria for compartmental models of disease transmission, *Math. Biosci.*, **180** (2002), 29–48. https://doi.org/10.1016/S0025-5564(02)00108-6
27. O. Diekmann, J. A. P. Heesterbeek, J. A. J. Metz, On the definition and the computation of the basic reproduction ratio r0 in models for infectious diseases in heterogeneous populations, *J. Math. Biol.*, **28** (1990), 365–382. https://doi.org/10.1007/BF00178324
28. A. F. Filippov, Differential equations with discontinuous righthand sides, *J. Math. Anal. Appl.*, **154** (1991), 377–390. https://doi.org/10.1016/0022-247X(91)90044-Z

29. V. Utkin, J. Guldner, J. X. Shi, *Sliding mode control in electro-mechanical systems*, 2^{nd} edition, CRC Press, Boca Raton, 2009. https://doi.org/10.1201/9781420065619

30. Y. A. Kuznetsov, S. Rinaldi, A. Gragnani, Non-smooth ecological systems with a switching threshold depending on the pest density and its rate of change, *Nonlinear Anal. Hybri.*, **42** (2021), 101094. https://doi.org/10.1016/j.nahs.2021.101094

31. Y. A. Kuznetsov, S. Rinaldi, A. Gragnani, One-parameter bifurcations in planar filippov systems, *Int. J. Bifurcat. Chaos*, **13** (2003), 2157–2188. https://doi.org/10.1142/S0218127403007874

32. A. A. Arafa, S. A. A. Hamdallah, S. Tang, Dynamics analysis of a filippov pest control model with time delay, *Commun. Nonlinear Sci.*, **101** (2021), 105865. https://doi.org/10.1016/j.cnsns.2021.105865

AIMS Press